Scientific Research Publishing

Materials Sciences and Applications, 2021, 12, 578-594
https://www.scirp.org/journal/msa
ISSN Online: 2153-1188
ISSN Print: 2153-117X

# Comparative Study of Structural, Optical and Electrical Properties of $SnO_2$ Thin Film Growth via CBD, Drop-Cast and Dip-Coating Methods

**Md. Tareq Rahman[1], Zubair Ahmed[1], Md. Johurul Islam[1], Kamaruzzaman[2], Mst. Toma Khatun[3], Md. Abdul Gafur[4], Md. Shahriar Bashar[4], Md. Monjarul Alam[1*]**

[1]Department of Electrical and Electronic Engineering, Islamic University, Kushtia, Bangladesh
[2]Department of Electrical and Electronic Engineering, Noakhali Science and Technology University, Noakhali, Bangladesh
[3]Atomic Energy Centre, Bangladesh Atomic Energy Commission, Dhaka, Bangladesh
[4]Bangladesh Council of Scientific and Industrial Research, Dhaka, Bangladesh
Email: *milon112000@gmail.com

**How to cite this paper:** Rahman, Md.T., Ahmed, Z., Islam, Md.J., Kamaruzzaman, Khatun, Mst.T., Gafur, Md.A., Bashar, Md.S. and Alam, Md.M. (2021) Comparative Study of Structural, Optical and Electrical Properties of $SnO_2$ Thin Film Growth via CBD, Drop-Cast and Dip-Coating Methods. *Materials Sciences and Applications*, **12**, 578-594.
https://doi.org/10.4236/msa.2021.1212038

**Received:** October 4, 2021
**Accepted:** December 6, 2021
**Published:** December 9, 2021



## Abstract

Tin oxide ($SnO_2$) thin films were deposited on glass substrate by Chemical Bath Deposition (CBD), Drop-Cast and Dip-Coating method. The thin films were post-annealed at 500˚C for 2 hours. The structural, optical, and electrical properties of the $SnO_2$ thin films were investigated by using XRD, FTIR, SEM, EDX, UV-Vis spectroscopy, and Electrometer experiment. The XRD patterns of $SnO_2$ thin films deposited on glass substrate by CBD method, Drop-Cast method and Dip-Coating method showed cubic, tetragonal and amorphous structures respectively. The FTIR spectrum exhibited the strong presence of $SnO_2$ with the characteristic vibrational mode of Sn-O-Sn. The SEM analysis was observed that the surface morphology of the thin films toughly depends on the deposition methods of the $SnO_2$ thin films. EDX measurement confirmed that the thin films are the composition of Tin (Sn) and Oxygen ($O_2$). The optical band gap of $SnO_2$ thin films deposited by CBD method, Drop-Cast method and Dip-Coating method is found to be 3.12 eV, 3.14 eV and 3.16 eV respectively. Thin films deposited by Dip-Coating method showed the highest band gap. The electrical results confirmed that the $SnO_2$ thin films are good conductors and pursued Ohm's Law. These properties of the $SnO_2$ thin films brand are appropriate for application in solar cell assembly, gas sensor devices and transparent electrodes of panel displays.

## Keywords

$SnO_2$ Thin Film, CBD, Drop-Cast and Dip-Coating Method, Electrical Property, Electrometer

## 1. Introduction

The development of modern society has become dependent on the progress of science and technology, which is not possible without technological improvement in the field of nano thin films. Nowadays microstructural and microelectronics components' demands rise in several sectors of science and technology which is significantly prolonged the arena of thin film research [1] [2]. Inorganic materials have been in focus because of their multifunctional advantages, for example, their solution-type processing, which allows deposition at room temperature and pressures. Inorganic thin films are used in different modern technological sectors such as coating interference filters, anti-reflection (A.R), solar cells, gas sensors, narrow band filters, diodes, biosensors, photoconductors, humidity sensors, IR detectors, temperature control of satellites, magnetic films, waveguide coatings, anticorrosive films, microelectronics devices, etc. [3] [4] [5] [6] [7]. $SnO_2$ thin film is very effective because of its well structural, superconducting films, optical and electrical properties. $SnO_2$ is one kind of n-type semiconductor that has been familiar to possess several outstanding physical properties such as high transmittance under visible range, high reflectivity for infrared light, high mechanical hardness, low electrical resistivity, wide band gap, excessive conductivity, great chemical stability, thermal stability and good environmental stability [8] [9]. The $SnO_2$ thin films have various effective applications such as in optoelectronic devices, including the gas sensors, solar cells, film resistors, heat-reflective mirror, liquid crystal display (LCD), light detectors, transparent conducting electrodes, electric conversion films, far-infrared detectors, biosensors and high-efficiency solar cells [10] [11] [12] [13] [14]. Generally, researchers have shown more interest in $SnO_2$-based films because $SnO_2$ thin films have a wide application in the modern engineering sectors. Mostly, the structural phases of $SnO_2$ are entirely different at various in constant of optics and subsist in the tetragonal or cubic phases, however, the atomic components are the same in materials. The phase is changed with producing method and annealing temperature. Overall discussion $SnO_2$ thin film is promising useable for optoelectronics and LPG (Liquefied petroleum gas) linkage detection because $SnO_2$ has high oxygen absorption power [1] [2]. The $SnO_2$ thin films can be deposited by several types of techniques such as vacuum evaporation, RF magnetron sputtering, Chemical bath deposition, pulsed laser deposition, chemical vapor deposition, pulsed electron beam deposition, spray pyrolysis, Dip-Coating, spin coating, Drop-Cast method, sol-gel and so on [15]-[20]. Having a vast variety of accessible alternatives, Chemical bath deposition method has been one of the most widely used techniques due to the thin films depositing by chemical bath deposition method has shown outstanding mechanical and physicochemical properties. Therefore, Chemical Bath Deposition method has gained recognition as a significant technique for thin film deposition of absolutely new kinds of oxide films. This technique is beneficial because of its marvelous quality, adherent to the substrate and pinhole free to acquire the thin films [21] [22]. The thickness of

the thin film can be easily controlled in a level of $\lambda/4$ of visible light at which the thin films can be appointed in optical instruments [23] [24] [25] [26]. Drop-Cast method is a very easy, fast and minimal waste system. Dip-Coating is much simpler, more economical and highly efficient. From the above review, it is considering that exploration of Structural, optical and electrical properties of $SnO_2$ thin films depositing by CBD, Drop-Cast and Dip-Coating methods using different deposition parameter and comparison of the different properties of $SnO_2$ thin films depositing by CBD, Drop-Cast and Dip-Coating methods which give us new aspects to find their suitable applications.

## 2. Materials and Methods

### 2.1. Preparation of Tin Oxide ($SnO_2$) Thin Films

The $SnO_2$ thin films were prepared by using $SnCl_2{\cdot}2H_2O$ (purity 98%), Sodium Hydroxide (NaOH) and Urea ($CO(NH_2)_2$) (purity 99%). The materials were obtained from Merck Germany. All of these raw materials ethanol, double distilled water were analytic reagent grade and were used without any purification. Impurities of the silica glass substrates may influence various properties of thin films. To remove the impurities, the glass substrates were dissolved in a solution where concentrated sulfuric acid ($H_2SO_4$) (purity 98%) was added to water. Then the substrates were rinsed with double distilled water. Again ethanol was used to clean the surface of the substrates properly. After that, the substrates were warmed-up in an oven at 80˚C for drying. These cleaned glass substrates were used to deposit thin films. In this research, the $SnO_2$ thin films were deposited via 1) Chemical Bath Deposition method; 2) Drop-Cast method; 3) Dip-Coating method.

**1) Chemical Bath Deposition method**

The $SnO_2$ thin film was prepared by CBD method using 200 ml 0.5M $SnCl_2{\cdot}2H_2O$ solution and 15 ml 1M $CO(NH_2)_2$ solutions. These two solutions were mixed together and stirring 30 minutes after that 200 ml of 1M NaOH was added and again stirring 30 minutes at room temperature and subsequently measured the pH value of this solution. The pH value of the solution was maintained at 12. Then the solution was sonicated for 10 minutes by Ultrasonic Cleaner. The cleaned glass substrate immersed in the solution at room temperature for 48 hours. After 48 hours of immersion, the $SnO_2$ thin film was formed on the glass substrate. The film was washed with double distilled water, dehydrated at a vacuum drier at 50˚C for 1 hour and annealed at 500˚C for 2 hours.

**2) Drop-Cast method**

The $SnO_2$ thin film was prepared by Drop-Cast method using 40 ml 1M $SnCl_2{\cdot}2H_2O$ solution and 3 ml 1M $CO(NH_2)_2$ solutions. These two solutions were mixed together and stirring 30 minutes and 1M NaOH was added drop wise to the solution until the pH value reached at 12, stirring the solution again for 30 minutes at 75˚C temperature. Then the cleaned glass substrate was kept on hot plate at 200˚C and 3 drops solution was given on the substrate and after

some time the substrate was removed from the hot plate and rinsed in double distilled water for removing the unwanted parts. This manner was repeated for 30 times and afterward a homogeneous $SnO_2$ thin film was formed on the substrate's surface. The film was dried at room temperature for 30 minutes and annealed at 500˚C for 2 hours.

**3) Dip Coating method**

The $SnO_2$ thin film was prepared by Dip coating method using 40 ml 1M $SnCl_2{\cdot}2H_2O$ solution and 3 ml 1M $CO(NH_2)_2$ solutions. These two solutions were mixed together and stirring 30 minutes and 1M NaOH was added drop wise to the solution until the pH value was reached at 12, stirring the solution again for 30 minutes at room temperature. Then the washed glass substrate was dipped into the solution by dip-coater, after some time the substrate withdrawal from the solution vertically at a constant speed, then it was dehydrating at room temperature and this manner was repeated for 30 times. After the removal of the substrate from the solution, a homogeneous film of $SnO_2$ was formed on the substrate's surface. The film was washed with double distilled water, dried at a vacuum drier at 50˚C for 1 hour and annealed at 500˚C for 2 hours.

In CBD method the glass substrate was kept into the solution for long time, when the concentration of $SnCl_2{\cdot}2H_2O$ was high, the particle was going down with time. For this reasonm the low concentration of $SnCl_2{\cdot}2H_2O$ was used for CBD method than other two methods. The different growth conditions of $SnO_2$ thin films for different methods are summarizes in Table 1.

## 2.2. Characterization Techniques

The structural properties of $SnO_2$ thin films were characterized by X-ray Diffractometer (D8 advance, Bruker, Germany). X-ray diffraction patterns were investigated from 20˚ to 70˚ with CuK$\alpha$ ($\lambda$ = 1.5406 Å) and scanning speed was 0.02 degree/sec. Peak intensities were recorded corresponding to their $2\theta$ degree values. The FTIR spectra were recorded using FT-IR/NIR spectrometer (Frontier, PerkinElmer, USA) in the transmission mode and the wavelength range was 400 - 4000 $cm^{-1}$. The $SnO_2$ film was scraped from the glass slide and made pellet for this measurement. Scanning Electron Microscope (Model JSM-6490LA, Jeol, Japan) was used to investigate the surface morphology and chemical composition

Table 1. Different growth conditions for different $SnO_2$ thin films.

| $SnO_2$ Thin Film | Reagent | Reducing agent | Complexing agent | pH | Deposition Temperature | Deposition time/times |
|---|---|---|---|---|---|---|
| CBD method | 200 ml of 0.5M $SnCl_2{\cdot}2H_2O$ | 1M NaOH | 1M $CO(NH_2)_2$ | 12 | Room Temperature | 48 hours |
| Drop-Cast method | 40 ml of 1M $SnCl_2{\cdot}2H_2O$ | 1M NaOH | 1M $CO(NH_2)_2$ | 12 | 200˚C | 30 times |
| Dip-Coating method | 40 ml of 1M $SnCl_2{\cdot}2H_2O$ | 1M NaOH | 1M $CO(NH_2)_2$ | 12 | Room Temperature | 30 times |

of $SnO_2$ thin films in secondary electron emission mode which applied voltage was 10 KV and distance was 8.5 mm. The optical properties of the samples were brought to pass with respect to plain glass substrate by using UV-Vis spectrophotometer (UV-1601, Shimadzu, Japan) in the range of 300 nm to 800 nm. The electrical properties were obtained by (6517B, Keithley, USA) Electrometer analysis system.

## 3. Results and Discussions

### 3.1. Structural Properties

The XRD diffraction technique was used to investigate the structural properties such as peak position, reflections plane, interplanar spacing, lattice parameter, crystallite size, dislocation density and strain. **Figure 1** shows the XRD patterns of $SnO_2$ thin films were deposited by CBD, Drop-Cast and Dip-Coating method. The film was deposited by CBD method is presented crystalline nature with cubic phase of tin oxide film. The strongest peak is at $2\theta = 31.69^\circ$ from diffraction pattern and other peaks are at 40.89˚ and 45.34˚ also observed reflections planes (hkl) corresponding to the peaks are (111), (210) and (211) respectively and the outcomes are almost similar to the reported data of JCPDS card No. 01-071-5329 [27].

The film was deposited by Drop-Cast method is presented crystalline nature with tetragonal phase of tin oxide. The strongest peak is at $2\theta = 26.51^\circ$ from diffraction pattern and other peaks are at 33.78˚ and 51.73˚ also observed reflections planes (hkl) corresponding to the peaks are (110), (101) and (211) respectively and the outcomes are almost similar to the reported data of JCPDS card No.041-1445 [28]. The tetragonal phase has shown more thermodynamically stable than cubic phase of $SnO_2$ thin films [29]. The film was deposited by Dip-Coating method is presented amorphous nature that means there are no significant peaks at the XRD result of this film.

From the literature it is observed that the $SnO_2$ crystals appeared at different annealing temperature, some are indicating above 550˚C [30], some are indicating at 500˚C [31] on the other hands some are indicating at 400˚C appeared some weak diffraction peaks and the peak intensity increases with temperature [32]. At this research, all the films are annealed at 500˚C for 2 hours due to observing all properties at the same condition. X-ray diffraction is a worthy method for obtaining the crystallite size of nano crystalline materials. The crystallite size (D) is measured by using the Scherrer formula [33].

$$D = K\lambda/\beta\cos\theta \tag{1}$$

where $D$ is the Crystallite size of nano-particles, $K$ is a constant related to crystallite shape and normally taken as 0.9, $\lambda$ is the wave length of X-ray (1.54056 Å), $\beta$ is the full width at half maximum (FWHM) intensity of the peak in radian, $\theta$ is the Bragg's diffraction angle. Average Crystallite sizes are given in **Table 2**. The strain ($\varepsilon$) of $SnO_2$ thin films are calculated by the following formula:

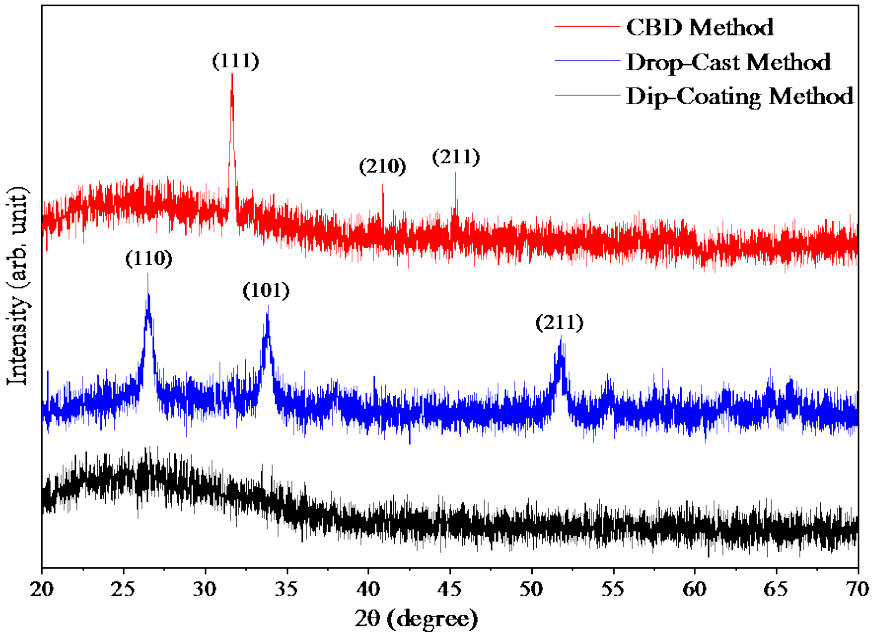


**Figure 1.** XRD patterns of $SnO_2$ thin films deposited by CBD, Drop-Cast and Dip-Coating method.

**Table 2.** Peak position, reflections plane, interplanar spacing ($d$), lattice parameter, average crystallite size, dislocation density and strain of $SnO_2$ thin films.

| Sample Name | Peak Position $2\theta$ (deg) | Reflections Plane (hkl) | Calculated Spacing $d$ (Å) | Standard Spacing $d$ (Å) | Calculated Lattice Parameter $a$, $b$ and $c$ | Standard Lattice Parameter $a$, $b$ and $c$ | Average Crystallite size $D$ (nm) | Dislocation Density ($\delta$) $\times 10^{-3}$ | Strain ($\varepsilon$) $\times 10^{-3}$ |
|---|---|---|---|---|---|---|---|---|---|
| CBD method (Cubic) | 31.69 | 111 | 2.82 | 2.82 | $a = b = c = 4.89$ | $a = b = c = 4.88$ | | 1.57 | 1.37 |
| | 40.89 | 210 | 2.18 | 2.18 | $a = b = c = 4.89$ | $a = b = c = 4.88$ | 25.01 | 3.90 | 2.16 |
| | 45.34 | 211 | 1.99 | 1.99 | $a = b = c = 4.89$ | $a = b = c = 4.88$ | | 0.87 | 1.02 |
| Drop-Cast method (Tetragonal) | 26.51 | 110 | 3.35 | 3.34 | $a = b = 4.75$, $c = 3.19$ | $a = b = 4.74$, $c = 3.20$ | | 5.29 | 2.52 |
| | 33.78 | 101 | 2.64 | 2.64 | $a = b = 4.75$, $c = 3.19$ | $a = b = 4.74$, $c = 3.20$ | 13.02 | 6.33 | 2.75 |
| | 51.73 | 211 | 1.76 | 1.76 | $a = b = 4.75$, $c = 3.19$ | $a = b = 4.74$, $c = 3.20$ | | 6.13 | 2.71 |

$$\varepsilon = \beta \cos\theta / 4 \tag{2}$$

where $\beta$ is the full-width at half-maximum of the preferential peak in radian, the measured values of strain are shown in Table 2. It is detected that the strain reductions with the increase of crystallite size. The dislocation density ($\delta$) is defined as the length of dislocation line per unit volume. The dislocation density ($\delta$) of the $SnO_2$ thin films are estimated from the following equation:

$$\delta = n / D^2 \tag{3}$$

where n is an element which is equivalent to unity giving minimum dislocation

density, usually $n$ is equal to 1 and $D$ is the crystallite size. The lattice constant for $SnO_2$ thin film is determined from the relation:

$$1/d^2 = \left(h^2/a^2 + k^2/b^2 + l^2/c^2\right) \quad (4)$$

where $d$ is the spacing between the crystal planes and ($hkl$) is a miller index. For cubic structure $a = b = c$ and for tetragonal $a = b$. The values of calculated lattice constants are marginally changed from standard for several orientations of the film. The XRD analyses for $SnO_2$ thin films deposited by different methods are summarized in Table 2.

## 3.2. Fourier Transform Infrared (FTIR) Spectroscopy

The FTIR spectrum of $SnO_2$ thin films are given in Figure 2. For CBD method, the potential peak at 540 $cm^{-1}$ is assigned to the fundamental Sn-O-Sn stretching vibration band and growing $SnO_2$ lattice [34]. The peak at 1016 $cm^{-1}$ represents the stretching vibrations of Sn-OH band. The absorption peak at around 1635 $cm^{-1}$ occurs due to the bending vibration of hydroxyl groups of molecular water. Furthermore, the broad peaks at 3453 $cm^{-1}$ observed which are assigned to the O-H stretching vibrations. For Drop-Cast method, the potential peak at 590 $cm^{-1}$ is assigned to the fundamental stretching vibrations for Sn-O-Sn [35]. The peak at around 1014 $cm^{-1}$ related to the characteristic of the Sn-OH stretching vibration band. The absorption peak at around 1588 $cm^{-1}$ represents the bending vibration of hydroxyl groups of molecular water. Besides, the broad peaks at 3441 $cm^{-1}$ identified which are ensured the stretching vibrations of O-H band. For Dip-Coating method, the potential peak at 567 $cm^{-1}$ is identified the fundamental stretching vibrations for Sn-O-Sn band and growing $SnO_2$ lattice. The absorption

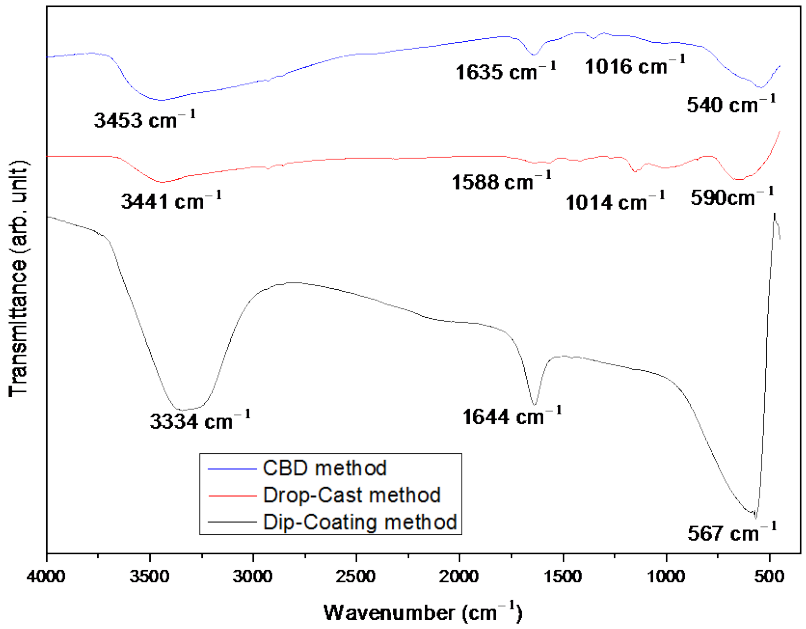


Figure 2. The FT-IR spectrum of $SnO_2$ thin films prepared by CBD, Drop-Cast and Dip-Coating method.

peak at around 1644 $cm^{-1}$ occurs due to the bending vibration of hydroxyl groups of molecular water. Furthermore, the broad peaks at 3334 $cm^{-1}$ identified which are ensured the O-H stretching vibration band. Thus the FTIR spectrum confirmed the presence of Sn-O-Sn bonds in the films.

### 3.3. Surface Morphology

Figure 3 represents the surface morphology of $SnO_2$ thin films were prepared by (a) CBD method; (b) Drop-Cast method; (c) Dip-Coating method on the glass substrate. These images indicate that the shape and morphology of $SnO_2$ thin films changes with methods. The particle sizes of the different $SnO_2$ thin films are measured using the ImageJ software from the SEM images. The average particle size for (a) CBD method; (b) Drop-Cast method; (c) Dip-Coating method are estimated ~1000 nm, ~500 nm and ~300 nm respectively. The particle sizes are little higher due to the high annealing temperature and layer by layer deposition method.

### 3.4. Energy Dispersive X-Ray Spectroscopy

Energy-dispersive X-ray is a popular systematic technique used to analyze elemental compositional investigation or chemical characterization of a sample. Figure 4 shows the EDX spectra and distribution and Table 3 shows the elements

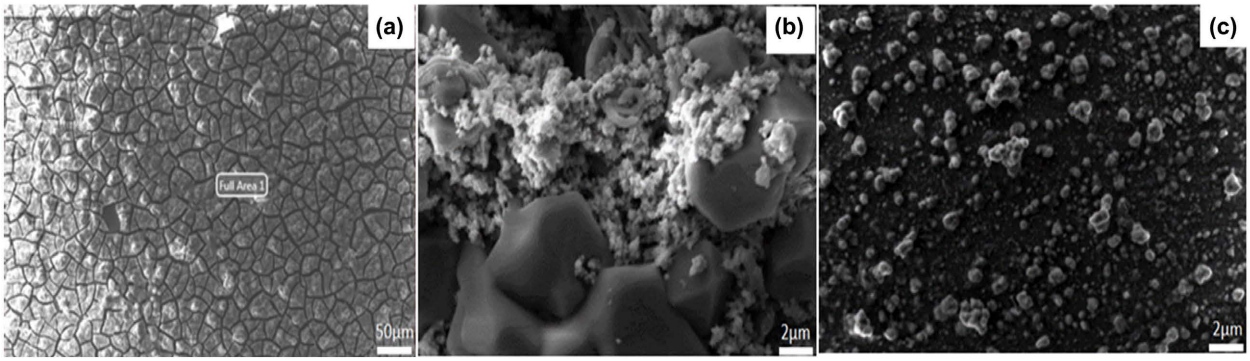


Figure 3. SEM images of $SnO_2$ thin films prepared by (a) CBD (25 KX), (b) Drop-Cast 10 KX) and (c) Dip-Coating (10 KX), method.

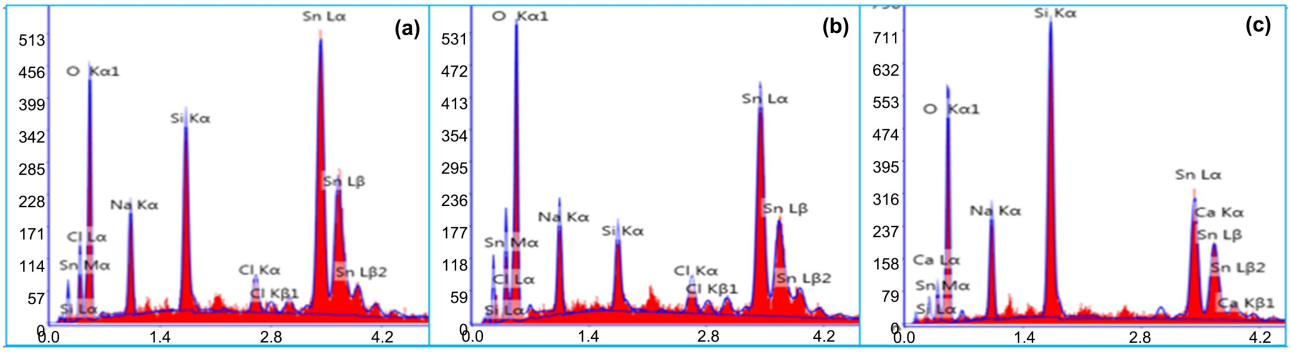


Figure 4. (a-c) shows the EDX spectra and distribution of elements for $SnO_2$ thin films were prepared by (a) CBD, (b) Drop-Cast and (c) Dip-Coating method deposited on glass substrate.

**Table 3.** Shows the EDX spectra elements weight and atomic percentages for $SnO_2$ thin films.

| Element | CBD method | | Drop-Cast method | | Dip-Coating method | |
|---|---|---|---|---|---|---|
| | Weight % | Atomic % | Weight % | Atomic % | Weight % | Atomic % |
| O | 20.19 | 52.53 | 29.13 | 51.03 | 20.19 | 50.53 |
| Na | 15.28 | 18.86 | 15.28 | 18.63 | 10.83 | 18.86 |
| Si | 20.55 | 06.78 | 20.55 | 20.51 | 4.76 | 6.78 |
| Cl | 02.47 | 03.09 | 3.36 | 2.35 | 2.74 | 3.09 |
| Sn | 61.48 | 20.74 | 31.68 | 7.48 | 61.48 | 20.74 |

weight and atomic percentages of elements of $SnO_2$ thin films. The quantification results in an atomic ratio of O/Sn close to 2.0 on the film surface in the case of CBD and Dip-Coating method and decreasing O/Sn atomic ratio with increasing sputtering time in the case of Drop-Cast method. It is well known that ion bombardment of $SnO_2$ leads to preferential sputtering of oxygen [36]. Therefore, a freshly prepared film in Drop-Cast method, where a sputter cleaning of the surface can be omitted, is best suited for a reliable composition examination [37].

**Figures 4(a)-(c)** and **Table 3** ensures the existence of Sn, Na, Cl, Si, and O in the $SnO_2$ thin films deposited by (a) CBD method, (b) Drop-Cast method and (c) Dip-Coating method and the elements were same in every deposition method. From the energy dispersive x-ray microanalysis measurement the existence of tin (Sn) and oxygen (O) is confirmed, besides tin (Sn) and oxygen (O) the existence of a little amount of other elements are due to the other elements in solution and glass substrate. The energy dispersive x-ray microanalysis measurement confirms that the films are indeed $SnO_2$ thin films.

### 3.5. Optical Properties

**Figure 5** shows the optical absorbance spectra of the $SnO_2$ thin films deposited by CBD, Drop-Cast and Dip-Coating method. It is observed that, the maximum absorbance happen in the ultra-violate region and then absorbance gradually decrease to visible region, reaches a maximum, and then absorbance gradually decreases up to for all the thin films. Above 400 nm, absorbance decreases slowly. All the $SnO_2$ thin films which are prepared by different methods are highly transparent in the visible region. The absorbance increases with increasing thickness of all the method prepared thin films. The wavelengths ($\lambda_{max}$) at maximum absorbance and maximum absorbance values corresponding to thin films of different thickness prepared by different methods are recorded in **Table 4**. The $\lambda_{max}$ does not shift much and absorbance increases with increasing the thickness of the films and scattering also increases with increasing the thickness of the films. The transmittance is high at visible region indicates that the films are relatively good homogeneous and formed at small nanometer-sized grains

**Table 4.** The wavelengths ($\Lambda_{max}$) at maximum absorbance, maximum absorbance values and optical direct band gap corresponding to different method prepared thin film of different thickness

| Method | Film Thickness, $d$ (nm) | Wavelength at maximum absorbance, $\Lambda_{max}$ (nm) | Maximum absorbance | Optical direct band Gap $E_g$ (eV) |
|---|---|---|---|---|
| CBD | 72.67 | 390 | 0.20 | 3.12 |
| Drop-Cast | 549 | 389 | 0.26 | 3.14 |
| Dip-Coating | 281 | 387 | 0.40 | 3.16 |

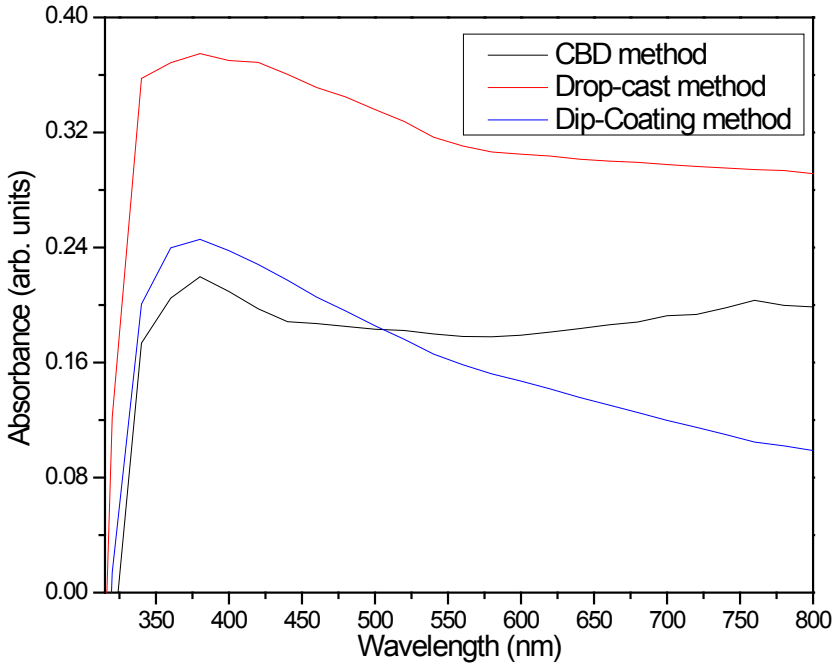


**Figure 5.** UV-Vis Absorption spectra of $SnO_2$ thin films prepared by CBD, Drop-Cast and Dip-Coating method.

which is opposite of absorbance [31]. The transmittance is high at visible region because of the reflectivity low and very low absorption. This happens due to the transition of electrons from valence band to conduction band with regard to optical interference effects [38] [39]. High transmittance at visible region is an important factors for the semiconducting material in a transparent device such as the $SnO_2$ thin films solar cell or transistor [31].

**Figure 5** shows the absorption spectra of the $SnO_2$ thin films. The maximum absorbance of all films is at ultraviolet region and decrease to visible region. This decrease in the absorbance indicates that the existence of optical band gap in the materials. In order to find out the optical band gap ($E_g$) of thin films, at first the absorption coefficient ($\alpha$) should be calculated using the following relation [40].

$$\alpha = (1/t) * \ln(1/T) \tag{5}$$

where, t is the thickness of the film and $T$ is the transmittance. The absorption coefficient ($\alpha$) decreases with increasing the value of transmittance. The optical

band gaps ($E_g$) of $SnO_2$ thin films are obtained using the Tauc relation [41].

$$\alpha h\nu = A\left(h\nu - E_g\right)n \tag{6}$$

where "$\alpha$" is the absorption coefficient, "$h\nu$" is the energy of absorbed photons, "$A$" is a proportionality constant and "$E_g$" is the optical band gap, and "$n$" is an index in regard to the density of state curves for the energy band. This "$n$" is obtained by the nature of the optical Transition involved in the absorption process. Analyses of the data have been made using $n = 1/2$ for direct transition and $n = 2$ for indirect transition [42].

The band gap of a semiconductor is related to the fundamental optical absorption edge. The plot of $(\alpha h\nu)^2$ vs. Energy (eV) for (direct transition) of $SnO_2$ thin films which were prepared by CBD method, Drop-Cast method and Dip-coating method are shown in **Figure 6** and the direct band gap energy have been obtained from the intercept on the energy axis after extrapolation of the straight

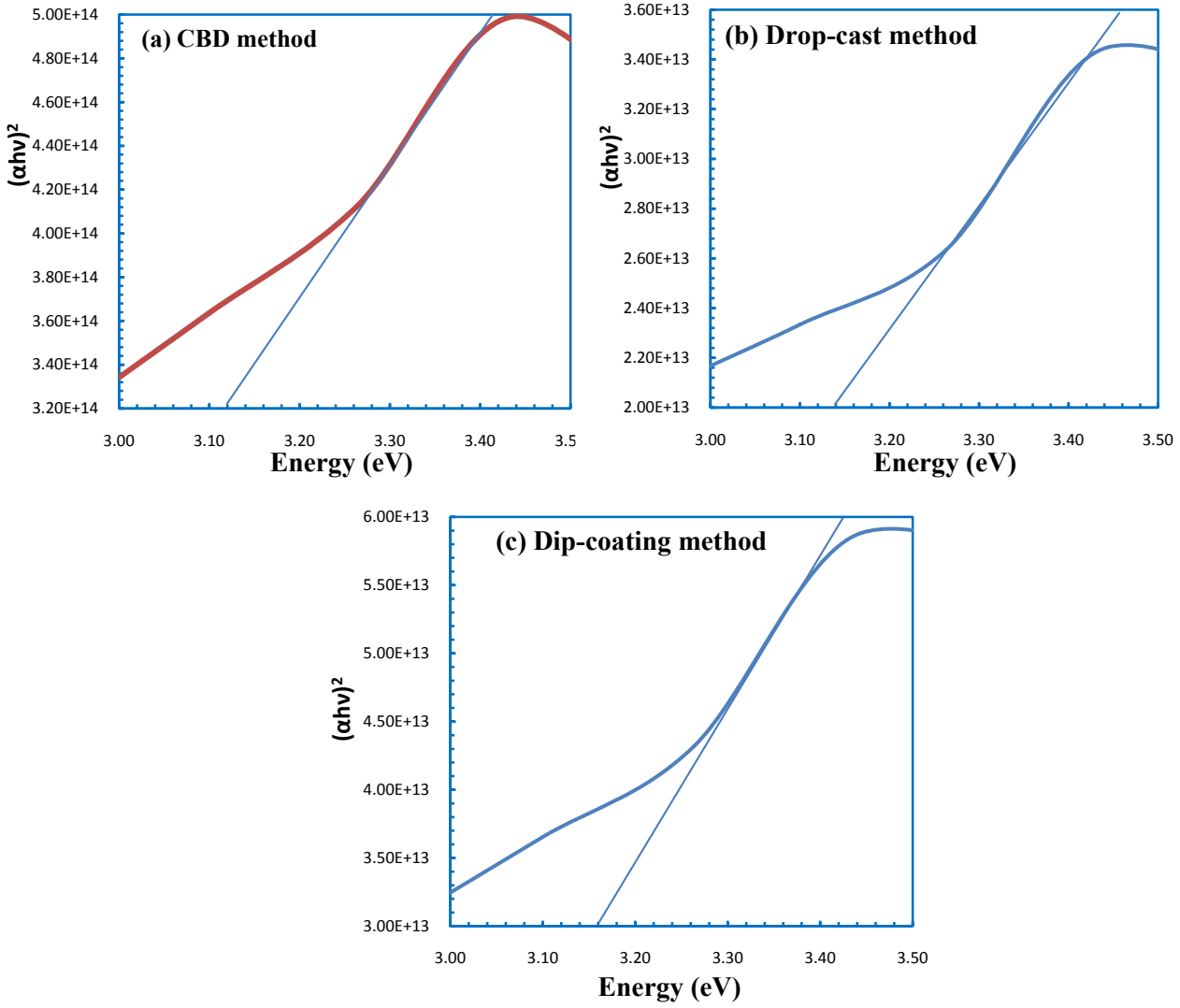


**Figure 6.** Plot of $(\alpha h\nu)^2$ vs. Energy (eV) for $SnO_2$ thin films prepared by (a) CBD method, (b) Drop-Cast method and (c) Dip-Coating method for estimation of band gap energy.

line section of $(ahv)^2$ vs. Energy (eV) curve [39]. The optical direct band gap of $SnO_2$ thin films which were prepared by (a) CBD, (b) Drop-Cast and (c) Dip-Coating methods are 3.12 eV, 3.14 eV and 3.16 eV respectively. These values are very close to the reported values [43]. The band gap of amorphous thin film is higher than crystalline thin films [44] and for the crystalline thin films the band gap is increasing with decreasing the crystallite size as the similarity in XRD results and increasing strain of the films [34].

### 3.6. Electrical Properties

Figure 7 shows the conductivity vs. temperature curve of $SnO_2$ thin films. From Figure 7, it is clear that the conductivity is increased with temperature. When the applied temperature was 10˚C the value of conductivity was around $2.2 \times 10^{-4}$ S/m, $7.3 \times 10^{-5}$ S/m and $2.6 \times 10^{-5}$ S/m respectively for CBD method, Drop-Cast method and Dip-Coating method. After increasing temperature conductivity also increases due to adventitious ions and/or electrons, at 100˚C value of conductivity was around $5.4 \times 10^{-4}$ S/m, $1.08 \times 10^{-4}$ S/m and $6.7 \times 10^{-5}$ S/m respectively for CBD method, Drop-Cast method and Dip-Coating method. Summaries the above it is confirmed that the conductivity is decreased from CBD method to Dip-Coating method because the surface morphology homogenously incorporates and crystallinity size higher in CBD method thin film [45]. For semiconductor, the conductivity increases with increasing the temperature [46].

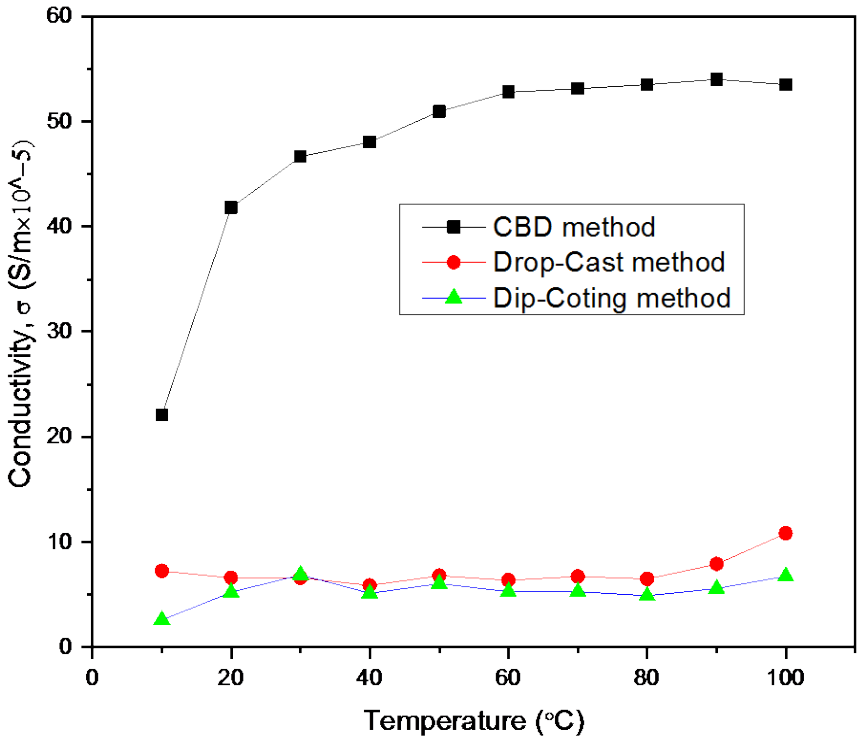


Figure 7. Conductivity vs. temperature curve of $SnO_2$ thin films prepared by CBD, Drop-Cast and Dip-Coating method.

## 4. Conclusion

$SnO_2$ thin films were successfully deposited on a glass substrate via different deposition methods and their effects on structural, optical and electrical properties have been investigated. The XRD patterns of $SnO_2$ thin films deposited by CBD, Drop-Cast and Dip-Coating methods are shown crystalline cubic phase, tetragonal phase and amorphous phase of tin oxide ($SnO_2$) respectively. The FT-IR spectrum confirmed the presence of Sn-O-Sn bonds in the films. SEM images show the surface morphology. EDX measurement ensured the existence of Sn and $O_2$ in the thin films. From the UV-visible spectroscopy measurements seen that the maximum absorbance of all films is at ultraviolet region and the absorbance decreases to the visible range. The optical direct band gap of $SnO_2$ thin films prepared by CBD, Drop-Cast and Dip-Coating methods are 3.12 eV, 3.14 eV and 3.16 eV respectively. The band gap of the amorphous thin film is higher than crystallite thin films and for the crystalline thin films, the band gap is increasing with decreasing the crystallite size and increasing strain of the films. The semiconducting behaviour of the $SnO_2$ thin films was confirmed from the electrical analysis. Finally, thin film prepared by CBD method shows better performance than the thin films prepared by Dip-Coating and Drop-Cast methods. The conductivity of thin film via CBD method is 5 times more than the thin films via Dip-Coating and Drop-Cast methods. So, its activation energy is more sensitive to active and it is useable as a gas sensor to identify the gas linkage.

## Acknowledgements

Authors would like to thank Islamic University Kushtia for providing the financial support under the UGC allocation, and Bangladesh Council of Scientific and Industrial Research, Dhaka, Bangladesh for providing the instrumental supports to carry out this work.

## Conflicts of Interest

The authors declare no conflicts of interest regarding the publication of this paper.

## References

[1] Prasad, S.V., Nainaparampil, J.J. and Zabinski, J.S. (2002) Tribological Behavior of Alumina Doped Zinc Oxide Films Grown by Pulsed Laser Deposition. *Journal of Vacuum Science & Technology*, **20**, 1738. https://doi.org/10.1116/1.1501567

[2] Lazar, M.A., Tadvani, J.K., Tung, W.S., Lopez, L. and Daoud, W.A. (2010) Nanostructured Thin Films as Functional Coatings. *Journal of Materials Science and Engineering*, **12**, Article ID: 012017. https://doi.org/10.1088/1757-899X/12/1/012017

[3] Eslamian, M. (2017) Inorganic and Organic Solution-Processed Thin Film Devices. *Journal of Nano-Micro Letters*, **9**, Article No. 3. https://doi.org/10.1007/s40820-016-0106-4

[4] Sarah, M.S.P., Musa, M.Z., Asiah, M.N. and Rusop, M. (2010) Electrical Conductivity Characteristics of TiO2 Thin Film. *IEEE* 2010 *International Conference on Elec-*

*tronic Devices*, *Systems and Applications* (*ICEDSA*), Kuala Lumpur, 11-14 April 2010, 361-364. https://doi.org/10.1109/ICEDSA.2010.5503040

[5] Zhao, X.Y., Liu, H.J. and Wang, M.Z. (2009) Polymer Dielectric Materials: Recent Advances in Dielectric Materials. Nova Science Publishers, New York, 323-368.

[6] Farahani, H., Wagiran, R. and Hamidon, M.N. (2014) Humidity Sensors Principle, Mechanism, and Fabrication Technologies: A Comprehensive Review. *Journal of MDPI*, **14**, 7881-7939. https://doi.org/10.3390/s140507881

[7] Thangaraju, B. (2002) Structural and Electrical Studies on Highly Conducting Spray Deposited Fluorine and Antimony Doped $SnO_2$ Thin Films from $SnCl_2$ Precursor. *Journal of Thin Solid Films*, **402**, 71-78. https://doi.org/10.1016/S0040-6090(01)01667-4

[8] Liu, Z.Q., Zhang, D.H., Han, S., Li, C., Tang, T., Jin, W., Liu, X.L., Lei, B. and Zhou, C.W. (2003) Laser Ablation Synthesis and Electron Transport Studies of Tin Oxide Nanowires. *Journal of Advance Materials*, **15**, 1754-1757. https://doi.org/10.1002/adma.200305439

[9] Vogt, P. and Bierwagen, O. (2018) Quantitative Subcompound-Mediated Reaction Model for the Molecular Beam Epitaxy of III-VI and IV-VI Thin Films: Applied to $Ga_2O_3$, $In_2O_3$, and $SnO_2$. *Journal of Physical Review Materials*, **2**, 120401(R). https://doi.org/10.1103/PhysRevMaterials.2.120401

[10] Liu, F.F., Shan, B., Zhang, S.F. and Tang, B.T. (2018) $SnO_2$ Inverse Opal Composite Film with Low-Angle-Dependent Structural Color and Enhanced Mechanical Strength. *Journal of Langmuir*, **34**, 3918-3924. https://doi.org/10.1021/acs.langmuir.7b04053

[11] Xiong, L.B., Guo, Y.X., Wen, J., Liu, H.R., Yang, G., Qin, P.L. and Fang, G.J. (2018) Review on the Application of $SnO_2$ in Perovskite Solar Cells. *Journal of Advance Function Materials*, **28**, Article ID: 1802757. https://doi.org/10.1002/adfm.201802757

[12] Wu, S.H., Li, Y.T., Luo, J.S., Lin, J., Fan, Y., Gan, Z.H. and Liu, X.Y. (2014) Pr and F Co-Doped $SnO_2$ Transparent Conductive Films with High Work Function Deposited by Ion-Assisted Electron Beam Evaporation. *Journal of Optics Express*, **22**, 4731-4737. https://doi.org/10.1364/OE.22.004731

[13] Yu, H., Yeom, H.I., Lee, J.W., Lee, K., Hwang, D., Yun, J., Ryu, J., Lee, J., Bae, S., Kim, S.K. and Jang, J. (2018) Superfast Room-Temperature Activation of $SnO_2$ Thin Films via Atmospheric Plasma Oxidation and Their Application in Planar Perovskite Photovoltaics. *Journal of Advance Materials*, **30**, Article ID: 1704825. https://doi.org/10.1002/adma.201704825

[14] Jiang, Q., Zhang, X.W. and You, J.B. (2018) $SnO_2$: A Wonderful Electron Transport Layer for Perovskite Solar Cells. *Journal of Small*, **14**, Article ID: 1801154. https://doi.org/10.1002/smll.201801154

[15] Liu, D., Wang, Q., Chang, H. and Chen, H. (1995) Variant Structure in Metal-Organic-Chemical-Vapor-Deposition-Derived $SnO_2$ Thin Films on Sapphire (0001). *Journal of Materials Research*, **10**, 1516-1522. https://doi.org/10.1557/JMR.1995.1516

[16] Ayouchi, R., Martin, F., Barrado, J., Martos, M., Morales, J. and Sánchez, L. (2000) Use of Amorphous Tin-Oxide Films Obtained by Spray Pyrolysis as Electrodes in Lithium Batteries. *Journal of Power Sources*, **87**, 106-111. https://doi.org/10.1016/S0378-7753(99)00435-8

[17] Baik, N., Sakai, G., Miura, N. and Yamazoe, N. (2000) Hydrothermally Treated Sol Solution of Tin Oxide for Thin-Film Gas Sensor. *Sensors and Actuators B*: *Chemi-*

*cal*, **63**, 74-79. https://doi.org/10.1016/S0925-4005(99)00513-4

[18] Deshpande, N., Vyas, J. and Sharma, R. (2008) Preparation and Characterization of Nanocrystalline Tin Oxide Thin Films Deposited at Room Temperature. *Journal of Thin Solid Films*, **516**, 8587-8593. https://doi.org/10.1016/j.tsf.2008.06.016

[19] Supothina, S. and De Guire, M. (2000) Characterization of $SnO_2$ Thin Films Grown from Aqueous Solutions. *Journal of Thin Solid Films*, **371**, 1-9. https://doi.org/10.1016/S0040-6090(00)00989-5

[20] Yu, S.H., Zhang, W.F., Li, L.X., Xu, D., Dong. H.L. and Jin, Y.X. (2013) Fabrication of P-Type SnO2 Films via Pulsed Laser Deposition Method by Using Sb as Dopant. *Applied Surface Science*, **286**, 417-420. https://doi.org/10.1016/j.apsusc.2013.09.107

[21] He, X.-W., Liu, W.-F., Zhu, C.-F. and Jiang, G.-S. (2011) CdS Thin Films Deposited by CBD Method on Glass. *Chinese Journal of Chemical Physics*, **24**, 471-476. https://doi.org/10.1088/1674-0068/24/04/471-476

[22] Mane, R.S. and Lokhande, C.D. (2000) Chemical Deposition Method for Metal Chalcogenide Thin Films. *Journal of Materials Chemistry and Physics*, **65**, 1-31. https://doi.org/10.1016/S0254-0584(00)00217-0

[23] Yang, S., Zhang, Y., Wang, L., Hong, S., Xu, J. and Chen, Y. (2006) Composite Thin Film by Hydrogen-Bonding Assembly of Polymer Brush and Poly(vinylpyrrolidone). *Journal of Langmuir*, **22**, 338-343. https://doi.org/10.1021/la051581e

[24] Tiwari, J.N., Meena, J.S., Chung-Shu, Wu, Tiwari, R.N., Chu, M.-C., Chang, F.-C. and Ko, F.-H. (2010) Thin-Film Composite Materials as a Dielectric Layer for Flexible Metal-Insulator-Metal Capacitors. *Journal of Physical Chemistry*, **3**, 1051-1056. https://doi.org/10.1002/cssc.201000118

[25] Sun, L., Qin, G., Huang, H., Zhou, H., Behdad, N., Zhou, W. and Ma, Z. (2010) Flexible High-Frequency Microwave Inductors and Capacitors Integrated on a Polyethylene Terephthalate Substrate. *Journal of Applied Physics*, **96**, Article ID: 013509. https://doi.org/10.1063/1.3280040

[26] Facchetti, A., Yoon, M.-H. and Marks, T.J. (2005) Gate Dielectrics for Organic Field-Effect Transistors: New Opportunities for Organic Electronics. *Journal of Advance Materials*, **17**, 1705-1725. https://doi.org/10.1002/adma.200500517

[27] Tewari, S. and Bhattacharjee, A. (2011) Structural, Electrical and Optical Studies on Spray-Deposited Aluminium-Doped ZnO Thin Films. *Pramana Journal of Physics*, **76**, 153-163. https://doi.org/10.1007/s12043-011-0021-7

[28] Scherrer, P. (1918) Nachrichten von der Gesellschaft der Wissenschaften zu Göttingen. *Mathematisch-Physikalische Klasse*, *Journal of Scientific Research*, **2**, 98-100.

[29] Carvalho, M.H., Pereirab, E.C. and de Oliveira, A.J.A. (2018) Orthorhombic $SnO_2$ Phase Observed Composite $(Sn_{1-x}Ce_x)O_2$ Synthesized by Sol-Gel Route. *Journal of RSC Advances*, **8**, 3958. https://doi.org/10.1039/C7RA12727H

[30] Kobayashia, T., Kimuraa, Y., Suzukia, H., Satoa, T., Tanigakia, T., Saitob, Y. and Kaitoa, C. (2002) Process of Crystallization in Thin Amorphous Tin Oxide Film. *Journal of Crystal Growth*, **243**, 143-150. https://doi.org/10.1016/S0022-0248(02)01445-8

[31] Lekshmy, S.S. and Joy, K. (2015) Effect of Different Dopants in Structural, Electrical and Optical Properties of SnO2 Thin Films Prepared by Sol Gel Technique. *International Journal of Engineering Research & Technology*, **3**.

[32] Li, Y.F., Yin, W.J., Deng, R., Chen, R., Chen, J., Yan, Q.Y., Yao, B., Sun, H.D., Wei, S.-H. and Wu, T. (2012) Realizing a $SnO_2$-Based Ultraviolet Light-Emitting Diode

via Breaking the Dipole-Forbidden Rule. *NPG Journal of Asia Materials*, **4**, e30. https://doi.org/10.1038/am.2012.56

[33] Kumara, G.R.A., Kaneko, S., Okuya, M. and Tennakone, K. (2002) Fabrication of Dye-Sensitized Solar Cells Using Triethylamine Hydrothiocyanate as a CuI Crystal Growth Inhibitor. *Journal of Langmuir*, **18**, 10493-10495. https://doi.org/10.1021/la020421p

[34] Baur, W.H. (1956) Über die Verfeinerung der Kristallstrukturbestimmung einiger Vertreter des Rutiltyps: $TiO_2$, $SnO_2$, $GeO_2$ und $MgF_2$. *Journal of Acta Crystallographica*, **9**, 515-520. https://doi.org/10.1107/S0365110X56001388

[35] Zhang, J.R. and Gao, L. (2004) Synthesis and Characterization of Antimony-Doped Tin Oxide (ATO) Nanoparticles. *Journal of Inorganic Chemistry Communications*, **7**, 91-93. https://doi.org/10.1016/j.inoche.2003.10.012

[36] Davide, B., Alberto, G., Maccato, C., Maragno, C. and Tondello, E. (2007) $TiO_2$ Thin Films by Chemical Vapor Deposition: An XPS Characterization. *Journal of Surface Science Spectra*, **14**, 27. https://doi.org/10.1116/11.20070902

[37] Baptista, A., Silva, F., Porteiro, J., Míguez, J. and Pinto, G. (2018) Sputtering Physical Vapour Deposition (PVD) Coatings: A Critical Review on Process Improvement and Market Trend Demands. *Coatings*, **8**, Article No. 402. https://doi.org/10.3390/coatings8110402

[38] Ramana, C.V., Smith, R.J. and Hussain, O.M. (2003) Grain Size Effects on the Optical Characteristics of Pulsed-Laser Deposited Vanadium Oxide Thin Films. *Journal of Physica Status Solidi* (*A*), **199**, R4-R6. https://doi.org/10.1002/pssa.200309009

[39] Yadav, A.A., Masumdara, E.U., Moholkarb, A.V., Neumann-Spallartc, M., Rajpured, K.Y. and Bhosaled, C.H. (2009) Electrical, Structural and Optical Properties of $SnO_2$:F Thin Films: Effect of the Substrate Temperature. *Journal of Alloys and Compounds*, **488**, 350-355. https://doi.org/10.1016/j.jallcom.2009.08.130

[40] Tauc, J., Grigorovici, R. and Vancu, A. (1966) Optical Properties and Electronic Structure of Amorphous Germanium. *Physica Status Solidi* (*B*), **15**, 627-637. https://doi.org/10.1002/pssb.19660150224

[41] Chowdhury, F.R., Choudhury, S., Hasan, F. and Begum, T. (2011) Optical Properties of Undoped and Indium-doped Tin Oxide Thin Films. *Journal of Bangladesh Academy of Sciences*, **35**, 99-111. https://doi.org/10.3329/jbas.v35i1.7975

[42] Banerjee, A.N. and Chattopadhyay, K.K. (2008) Reactive Sputtered Wide-Bandgap p-Type Semiconducting Spinel $AB_2O_4$ and Delafossite $ABO_2$ Thin Films for "Transparent Electronics". In: Depla, D. and Maheiu, S., Eds., *Reactive Sputter Deposition*, Springer, Berlin, Heidelberg. https://doi.org/10.1007/978-3-540-76664-3_12

[43] Ebrahimiasl, S., Yunus, W., Kassim, A. and Zainal, Z. (2011) Synthesis of Nanocrystalline $SnO_x$ (x = 1-2) Thin Film Using a Chemical Bath Deposition Method with Improved Deposition Time, Temperature and pH. *Journal of MDPI*, **11**, 9207-9216. https://doi.org/10.3390/s111009207

[44] Yildiz, A., Cansizoglu, H., Abdulrahman, R. and Karabacak, T. (2015) Effect of Grain Size and Strain on the Bandgap of Glancing Angle Deposited AZO Nanostructures. *Journal of Materials Science*: *Materials in Electronics*, **26**, 5952-5957. https://doi.org/10.1007/s10854-015-3167-0

[45] Matysiak, W., Tański, T., Smok, W. and Polishchuk, O. (2020) Synthesis of Hybrid Amorphous/Crystalline $SnO_2$ 1D Nanostructures: Investigation of Morphology, Structure and Optical Properties. *Scientific Reports*, **10**, Article No. 14802. https://doi.org/10.1038/s41598-020-71383-2

[46] Sawickia, B., Tomaszewiczb, E., Piatkowskab, M., Grona, T., Dudaa, H. and Górnya, K. (2016) Correlation between the Band-Gap Energy and the Electrical Conductivity in $MPr_2W_2O_{10}$ Tungstates (Where M = Cd, Co, Mn). *Acta Physica Polonica A*, **129**, 94. https://doi.org/10.12693/APhysPolA.129.A-94